



A Journal of the Gesellschaft Deutscher Chemiker

# Angewandte Chemie

GDCh

International Edition

www.angewandte.org

## Accepted Article

**Title:** "Dry" Chemistry of Ferrate(VI): A Solvent-free Mechanochemical Way for Versatile Green Oxidation

**Authors:** Zhao-yang Zhang, Deyang Ji, Wenting Mao, Yu Cui, Qing Wang, Lu Han, Hongliang Zhong, Zhongming Wei, Yixin Zhao, Kasper Nørgaard, and Tao Li

This manuscript has been accepted after peer review and appears as an Accepted Article online prior to editing, proofing, and formal publication of the final Version of Record (VoR). This work is currently citable by using the Digital Object Identifier (DOI) given below. The VoR will be published online in Early View as soon as possible and may be different to this Accepted Article as a result of editing. Readers should obtain the VoR from the journal website shown below when it is published to ensure accuracy of information. The authors are responsible for the content of this Accepted Article.

**To be cited as:** *Angew. Chem. Int. Ed.* 10.1002/anie.201805998  
*Angew. Chem.* 10.1002/ange.201805998

**Link to VoR:** <http://dx.doi.org/10.1002/anie.201805998>  
<http://dx.doi.org/10.1002/ange.201805998>

# “Dry” Chemistry of Ferrate(VI): A Solvent-free Mechanochemical Way for Versatile Green Oxidation

Zhao-Yang Zhang, Deyang Ji, Wenting Mao, Yu Cui, Qing Wang, Lu Han, Hongliang Zhong, Zhongming Wei, Yixin Zhao, Kasper Nørgaard, and Tao Li\*

**Abstract:** The +6 oxidation state of iron generally exists in the form of ferrate(VI) with high redox potential and environmentally friendly nature. Although ferrate(VI) has been known for over a century, its chemistry is still limited to the solvent-based reactions that suffers from the insolubility/instability of this oxidant and the environmental issues caused by hazardous solvents. Herein, we explore the solvent-free reactivity of ferrate(VI) under mechanical milling, revealing that its strong oxidizing power is accessible in the “dry” solid state towards a broad variety of substrates, e.g., aromatic alcohols/aldehydes and carbon nanotubes. More significantly, solvent-free mechanochemistry also reshapes the oxidizing ability of ferrate(VI) due to the underlying solvent-free effect and the promotive mechanical actions. This study opens up a new chemistry of ferrate(VI) with promising application in green oxidative transformation of both organic and inorganic substrates.

Compounds containing elements in extraordinarily high oxidation states are of fundamental interest because of their unique and intriguing reactivities.<sup>[1]</sup> Given the role of high-valent iron in oxidation chemistry,<sup>[2]</sup> ferrate(VI) (commonly  $K_2FeO_4$ ) with its central Fe in the highest +6 state has received special attention.<sup>[3]</sup> The hexavalent iron endows ferrate(VI) with very strong oxidizing ability (higher redox potentials than those of most traditional oxidants, e.g.,  $KMnO_4$ ,  $K_2Cr_2O_7$ ,  $HNO_3$ ,  $Cl_2$ ,  $H_2O_2$ ,  $O_3$ ),<sup>[4]</sup> and its nontoxic reduction product  $Fe^{III}$  and the abundance of iron on earth make it a green and sustainable oxidant.<sup>[3,4a]</sup>

In the past few decades, many efforts have been devoted to employing ferrate(VI) as an oxidizing agent for green organic synthesis,<sup>[3b,5]</sup> high-capacity battery,<sup>[6]</sup> and water purification,<sup>[3a,4,7]</sup> which greatly improved our understanding on its reactivity and performance. Recently, ferrate(VI) was also utilized for the oxidation of carbon materials, for example, modification of carbon nanotubes (CNTs)<sup>[8]</sup> and preparation of graphene oxides.<sup>[9]</sup> In these studies,  $K_2FeO_4/H_2SO_4$  was suggested as a

relatively green oxidation system to replace the traditional  $HNO_3/H_2SO_4$  or  $KMnO_4/H_2SO_4$ . At the same time, concern was also raised regarding the instability of  $K_2FeO_4$  in acidic  $H_2SO_4$  environment that could result in the loss of its oxidizing power.<sup>[10]</sup>

To date, to the best of our knowledge, ferrate(VI) chemistry is limited to the solvent-based reactions. Specifically, organic solvents, aqueous media, and *conc.*  $H_2SO_4$  were used for organic synthesis, pollutant degradation, and treating carbon materials, respectively. However, solvent-based chemistry suffers from the following problems. First, ferrate(VI) ion is intrinsically unstable in aqueous solutions, where it readily oxidizes  $H_2O$  and decomposes to  $Fe^{III}$ , and the self-decay is sensitive to solution environment, e.g., pH, temperature, concentration, impurity and coexisting aqueous species.<sup>[11]</sup> In particular, high redox potentials up to 2.2 V can be theoretically obtained at low pH, but its rapid decomposition makes the fascinating oxidizing power inaccessible in real applications. Second, ferrate(VI) solid is insoluble in organic solvents,<sup>[5a,c]</sup> thus most of its oxidizing capability is actually “hidden” inside the solid structure and the accessible surface will be gradually passivated by the resultant  $Fe^{III}$  during reaction, which are undesirable for efficient/effective oxidative transformations. Third, the hazardous organic solvents (e.g., benzene, cyclohexane, pentane) and corrosive *conc.*  $H_2SO_4$  for ferrate(VI) oxidation are of great environmental and health concern, thus their usage inconsequently goes against the spirit of green chemistry.<sup>[12]</sup>

To address the above issues, a challenging task is to establish a new chemistry of ferrate(VI) where: 1) the oxidant displays the desired reactivity; 2) it can be utilized in the stable form; 3) the problem of insolubility is circumvented; and 4) genuinely green oxidation will be achieved. In this work, we explore the solvent-free reactions of ferrate(VI), as depicted in Fig. 1a. Ferrate(VI) salt keeps stable in the as-prepared solid state, but its intrinsic reactivity in the absence of solvent remains unknown. The structure of  $K_2FeO_4$  solid was characterized with X-ray diffraction (Fig. S3), scanning and transmission electron microscopy (SEM and TEM), revealing that the purple-black crystalline powder was composed of large plate crystals on the scale of several to dozens of  $\mu m$  (Fig. 1b,S4). For solid-state reactions of such crystalline oxidizer, the reactivity is predefined by the exposed facets. Selected area electron diffraction (SAED) patterns were obtained on ferrate(VI) for the first time, which confirmed the single-crystalline nature of the individual plates and disclosed that  $K_2FeO_4$  crystals predominantly exposed the low-index {001} planes (top and bottom facets) with side planes of {200} and {010} jointed by small {210}, as shown in Fig. 1c. Considering its large crystal size and that crystal particles preferentially expose the planes with low surface energy (and expected low reactivity),<sup>[13]</sup> such as the {001} planes of  $K_2FeO_4$ , mechanical milling was employed to crush the original crystals and continually generate reactive fracture surface to participate into redox. Another merit of mechanochemistry is the ability to promote reactions under solvent-free conditions,<sup>[14]</sup> which is particularly beneficial for reactants like  $K_2FeO_4$  that lack

[\*] Z. Y. Zhang, W. Mao, Q. Wang, Prof. L. Han, Prof. H. Zhong, Prof. T. Li

School of Chemistry and Chemical Engineering and Key Laboratory of Thin Film and Microfabrication (Ministry of Education), Shanghai Jiao Tong University, Shanghai 200240, China  
E-mail: litao1983@sjtu.edu.cn

D. Ji

Center for Nanotechnology, Heisenbergstraße 11, 48149 Münster, Germany

Y. Cui, Prof. Z. Wei

State Key Laboratory of Superlattices and Microstructures, Institute of Semiconductors, Chinese Academy of Sciences, Beijing 100083, China

Prof. Y. Zhao

School of Environmental Science and Engineering, Shanghai Jiao Tong University, Shanghai 200240, China

Prof. K. Nørgaard

Nano-Science Center & Department of Chemistry, University of Copenhagen, Universitetsparken 5, Copenhagen 2100, Denmark

Supporting information for this article is given via a link at the end of the document.

solubility in media.

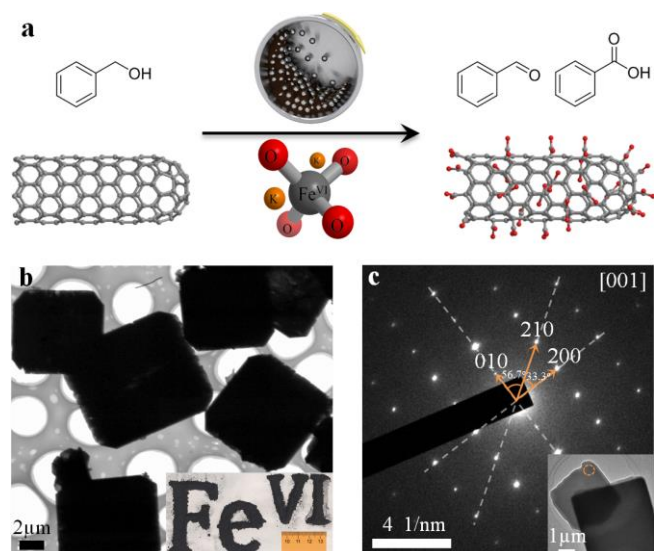


**Figure 1.** (a) Schematic of solvent-free mechanochemical reactions of  $K_2FeO_4$ . (b) TEM images of  $K_2FeO_4$  crystals (inset: a photo of  $K_2FeO_4$  powder arranged into a  $Fe^{VI}$  symbol). (c) An indexed SAED pattern viewed along [001] zone axis belonging to the circled area of a thin sheet (inset).

In our initial study, benzyl alcohol was used as a model substrate to probe the solvent-free reactivity of ferrate(VI) under ball milling (Fig. 2a,b). Benzyl alcohol oxidation by ferrate(VI) is well studied within the scope of “wet” chemistry, which clearly indicates that in organic phases the reaction 1) proceeds sluggishly with ferrate(VI) alone but efficiently when appropriate catalysts are used in combination and 2) only produces benzaldehyde without overoxidation to benzoic acid, as reported by Delaude and Laszlo (Fig. 2c).<sup>[5a]</sup> As shown in Fig. 2a, milling treatment of a mixture of  $K_2FeO_4$  and benzyl alcohol (molar ratio 2:1) led to distinct color change from black to yellow within 2 h, consistent with the reduction of  $Fe^{VI}$  to  $Fe^{III}$ . The time evolution of organic products monitored by GC-MS was presented in Table 1. The reaction was quite fast, with 82% alcohol consumed at 30 min. Benzaldehyde was produced as expected but its content started to drop at ~30 min due to further conversion to benzoic acid. The starting alcohol and

**Table 1.** Time evolution of benzyl alcohol during  $K_2FeO_4$  oxidation.

Time/min	$C_6H_5CH_2OH/mol\%$	$C_6H_5CHO/mol\%$	$C_6H_5COOH/mol\%$
0	100	0	0
15	60.2	39.8	0
30	18.0	54.3	27.7
60	13.5	38.1	48.4
120	2.4	5.5	92.1
180	0.4	1.2	98.4

intermediate aldehyde were almost fully oxidized to the acid at 3 h. The overall reaction process, described by Fig. 2b, disclosed the strong and unexpected reactivity of ferrate(VI) in the “dry” solid state, which enables 1) rapid oxidation of benzyl alcohol to benzaldehyde without the need of catalyst and 2) aldehyde-to-acid conversion to be accessible and efficient, in striking contrast to the traditional solvent-based chemistry.



**Figure 2.** (a) Photos of  $K_2FeO_4$ /benzyl alcohol reaction system before and after ball milling. (b-c) Comparison of  $K_2FeO_4$  oxidation of benzyl alcohol by solvent-free mechanical milling and traditional solvent-based route.<sup>[5a]</sup>

To understand this solvent-free reactivity, a control experiment on benzyl alcohol oxidation without ball milling was performed. Specifically, the solid-state  $K_2FeO_4$ /benzyl alcohol mixture was left to stand at  $-30^\circ C$ . Surprisingly, a high exotherm was observed upon mixing and a considerable amount of aldehyde (8%) and acid (32%) were produced after 3 h standing. On the other hand, stirring the reactants in pentane only yielded 12% of benzaldehyde without benzoic acid, in agreement with Fig. 2c. These results indicated that ferrate(VI) crystals themselves in the absence of solvents had intrinsically strong reactivity while the milling force could further promote the reactions to be more efficient and complete. *Solvent-free effect* obviously played a fundamental role in effective oxidation and reshaped the reactivity of ferrate(VI). The fact that oxidation could proceed more effectively without solvents is a rather interesting phenomenon. Future theoretical work on the interactions of the exposed facets of  $K_2FeO_4$  with organics in the presence/absence of solvents would provide more in-depth understanding on this issue.

Ferrate(VI) has been well-documented as a selective oxidant that does not oxidize aldehydes into acids.<sup>[5,15]</sup> However, under solvent-free condition a high reactivity towards aldehydes was brought into play. To further demonstrate this point, we conducted reactions with a series of benzaldehydes listed in Table S1. Again, the dark color of  $K_2FeO_4$  faded and turned to yellow with the progress of reactions (Fig. S5). Generally, the transformations were nearly quantitative within several hours with a slight excess of  $K_2FeO_4$ , giving the corresponding acids in high yields. Notably, dicarboxylic products were also generated from methyl substituted aldehydes (entries 2~4, Table S1),

indicating the deep conversion of methyl groups following the process of  $-\text{CH}_3 \rightarrow -\text{CH}_2\text{OH} \rightarrow -\text{CHO} \rightarrow -\text{COOH}$ . Besides, without the addition of  $\text{K}_2\text{FeO}_4$  or using  $\text{Fe}^{\text{III}}$  ( $\text{Fe}_2\text{O}_3$  and  $\text{FeCl}_3$ ) as oxidants, only small amounts of benzoic acid formed (Fig. S6).

Based on the above, we extended the solvent-free ferrate(VI) chemistry to the oxidation of inorganic carbon materials, including multi-walled and single-walled CNTs (MWNTs and SWNTs), in order to 1) verify the versatility of such ferrate(VI) oxidation, 2) investigate the reactivities of ferrate(VI) towards different carbon structures and 3) achieve genuinely green oxidation compared to the  $\text{K}_2\text{FeO}_4/\text{H}_2\text{SO}_4$  method.<sup>[8,9]</sup>

The oxidation was found very efficient for MWNTs. The surface O/C ratio, detected by X-ray photoelectron spectroscopy (XPS, surface semi-quantitative), increased from 3.5% to 11.3% after only 2 h (Fig. 3a), and the bulk O/C ratio measured by elemental analysis (EA) was improved from 1.6% to 4.1%. Effective carboxylation at the surface was achieved with evident  $-\text{COOH}$  peaks in C 1s and O 1s spectra (Fig. 3b,c) as well as infrared adsorption at  $\sim 1740\text{ cm}^{-1}$  (Fig. S12). 1 h reaction also led to obvious oxidation/carboxylation, only with a little lower degree (Fig. 3e,S7 and Table S2). Ball milling without  $\text{K}_2\text{FeO}_4$  for 4 h gave negligible oxidizing effects (Fig. S8), confirming that effective oxidation resulted from the reaction with  $\text{K}_2\text{FeO}_4$ . Thermal gravimetric analysis coupled with mass spectrometry (TGA-MS, bulk quantitative) showed the  $-\text{COOH}$  content (see Fig. 3d for the results of 2 h sample) of 0.632 and 0.729 mmol/g after 1 and 2 h oxidation, respectively, remarkably elevated

relative to the raw material (0.295 mmol/g) (Fig. 3e,S10). The values are even higher than traditional  $\text{KMnO}_4/\text{H}_2\text{SO}_4$  oxidation on the same MWNTs by the supplier (0.569 mmol/g, product code *TNMC2*).<sup>[16]</sup> As a result of the dense  $-\text{COOH}$ , the  $\text{K}_2\text{FeO}_4$  oxidized MWNTs exhibited excellent aqueous dispersibility of up to 4.6 and 4.7 mg/ml for 1 and 2 h products, respectively (Fig. 3f). As a comparison, heavily oxidized ultrashort MWNTs produced by Hummers method were reported to be 2.5 mg/ml.<sup>[17]</sup> Generally, Hummers oxidation produces mainly epoxy, hydroxyl and carbonyl groups but relatively low quantities of carboxyls.<sup>[18]</sup>

SWNTs can also be effectively oxidized by  $\text{K}_2\text{FeO}_4$ , only requiring longer treatment. As indicated by the water dispersibility (Fig. 3g), 2 or 4 h treatment could not introduce enough functional groups to the surface, but substantial modification was achieved at 8 h. The resulting sample had a much higher O/C ratio than raw SWNTs (Fig. 3h) and the  $-\text{COOH}$  peak was clearly discernable from C 1s spectrum (Fig. 3i). To further improve the oxidation degree, the reaction was prolonged to 12 and 18 h, and the solubility was increased from 0.34 (8 h) to 0.44 and 0.87 mg/ml, respectively (Fig. 3j). These values are moderate compared to the data of hydrophilic SWNTs in literatures (Table S5). As a further comparison, the solubility of "high-functionality" SWNT-COOH product (*P3-SWNT, Carbon Solutions*),<sup>[19]</sup> produced by  $\text{HNO}_3$  refluxing, is determined as 0.7 mg/ml.<sup>[20]</sup> The 18 h sample was further analyzed by XPS and TGA-MS, showing an apparent higher O/C ratio of 14.1% and  $-\text{COOH}$  content of up to 1.43 mmol/g (Fig. S13,S14).

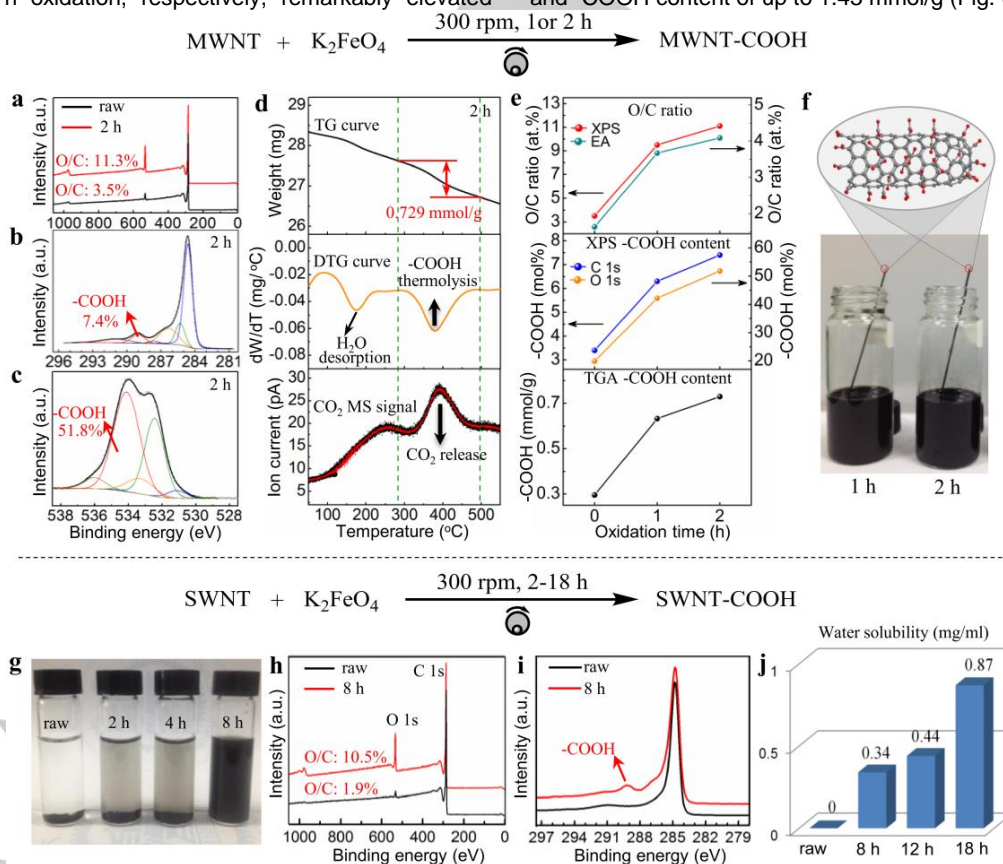
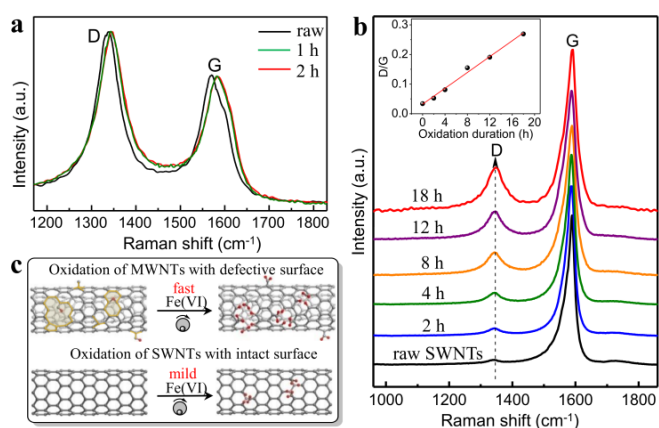


Figure 3. (a-f) Oxidation results of MWNTs: (a) XPS survey spectra, (b-c) C 1s and O 1s spectra, (d) TGA-MS profile, (e) a summary of O/C ratio and  $-\text{COOH}$  content, (f) saturated water dispersions of oxidized MWNTs inserted with 0.3 mm-diameter glass capillaries and structural model of a carboxylated tube. (g-j) Oxidation results of SWNTs: (g) photos 0.1 mg/ml SWNT in water sonicated for 5 min and settled overnight, (h-i) XPS survey and C 1s spectra, (j) water solubility.



**Figure 4.** Raman spectra of (a) MWNTs and (b) SWNTs (inset: liner fitting of  $I_D/I_G$  with reaction time). (c) Different oxidation processes on defective and perfect surface (the yellow lines mark the defective sites).

The different reactivities of ferrate(VI) towards MWNTs and SWNTs originated from their different surface structures. The MWNTs used in this study was found highly defective evidenced by its intense D peak in Raman spectrum (Fig. 4a), while the surface of starting SWNTs was nearly perfect (tiny D band in Fig. 4b).  $K_2FeO_4$  exhibited high reactivity towards the surface defects, such as C-H/C-OH dangling bonds and strained C=C bonds, and converted them rapidly into oxygenated groups like -COOH, thus affording a high oxidation degree. Large upshifts in D (+ 5  $cm^{-1}$ ) and G bands (+ 10  $cm^{-1}$ ) were observed after MWNT oxidation (Fig. 4a), arising from the “doping” effect by the high density of oxygenated groups.<sup>[21]</sup> On the other hand, the defect degree, measured by the relative intensity of D to G band ( $I_D/I_G$ ), remained substantially unchanged from 1.34 (raw MWNTs) to 1.35 (1 h) and 1.36 (2 h). Thus, ferrate(VI) oxidation occurred primarily at the defects without affecting the overall graphitic structure (Fig. 4c), which are advantageous over many classical approaches where the oxidizing species are aggressive towards CNT skeleton and thus high-level functionalization is at the expense of structural damage.<sup>[8,18a,22]</sup> The nondestructive oxidation was also supported by TEM images with almost identical features before and after the oxidation (Fig. S17).

The surface oxidation of SWNTs involved breaking the highly inert C=C bonds in lattice (Fig. 4c), as reflected by the gradual intensification of D band (Fig. 4b). The  $I_D/I_G$  was found to increase almost linearly with time (Fig. 4b inset), implying that, although the reaction was not rapid, its mildness allowed the oxidation degree to be controlled by adjusting the reaction time. In this fashion, a good oxidation degree can be obtained before destroying the electronic structure, which was verified by Vis-NIR results in Fig. S18, and the TEM results of SWNTs subjected to various reaction times (Fig. S19) also supported the mildness of such oxidative treatment. Presumably, the mechanical ferrate(VI) oxidation of SWNTs follows one of the two mechanisms: 1) direct oxidation of C=C bonds by  $K_2FeO_4$  activated by mechanical force or 2) generation of defects by milling force with subsequent *in situ* oxidation by the oxidizer. No matter which mechanism dominates, it is clear that, in either case, mechanical force and solvent-free reactivity of ferrate(VI)

play synergistic roles. In addition, the physical “crushing” and “mixing” roles of milling force was verified by SEM in Fig. S21.

In summary, ferrate(VI) solid under solvent-free conditions displays intrinsically strong and unexpected oxidizing power, which can be readily harnessed and promoted by mechanochemistry for green oxidative transformation of both organic and inorganic substrates. These findings open up a new chemistry of ferrate(VI), which circumvents the problems associated with the current solvent-based route and offers the opportunity to uncover many new knowledge of ferrate(VI) from both fundamental research and application aspects.

## Acknowledgements

The authors acknowledge the financial support from National Natural Science Foundation of China (51673114), Shanghai Science and Technology Committee (17ZR1447300) and National Key Research and Development Program of China (2017YFA0207500). We thank the Instrumental Analysis Center of SJTU. We are grateful to Dr. Jin-Long Pan for providing the GC-MS tests.

**Keywords:**  $K_2FeO_4$  • green chemistry • ball milling • carbon materials

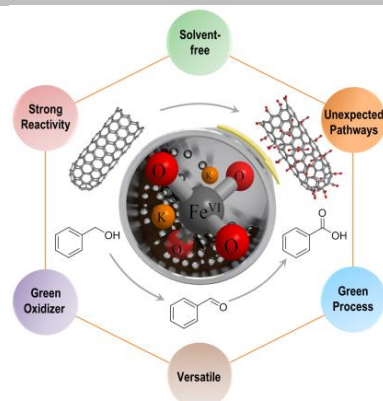
- [1] a) S. Riedel, M. Kaupp, *Coord. Chem. Rev.* **2009**, 253, 606; b) G. Wang, M. Zhou, J. T. Goettel, G. J. Schrobilgen, J. Su, J. Li, T. Schlöder, S. Riedel, *Nature* **2014**, 514, 475.
- [2] a) J. Hohenberger, K. Ray, K. Meyer, *Nat. Commun.* **2012**, 3; b) P. J. Chirik, *Angew. Chem. Int. Edit.* **2006**, 45, 6956; c) M. Ghosh, K. K. Singh, C. Panda, A. Weitz, M. P. Hendrich, T. J. Collins, B. B. Dhar, S. Sen Gupta, *J. Am. Chem. Soc.* **2014**, 136, 9524.
- [3] a) V. K. Sharma, R. Zboril, R. S. Varma, *Acc. Chem. Res.* **2015**, 48, 182; b) V. K. Sharma, L. Chen, R. Zboril, *ACS Sustain. Chem. Eng.* **2016**, 4, 18.
- [4] a) V. K. Sharma, *Adv. Environ. Res.* **2002**, 6, 143.; b) J. Q. Jiang, B. Lloyd, *Water Res.* **2002**, 36, 1397.
- [5] a) L. Delaude, P. Laszlo, *J. Org. Chem.* **1996**, 61, 6360; b) S. Caddick, L. Murtagh, R. Weaving, *Tetrahedron* **2000**, 56, 9365; c) H. Song, Z. G. Li, B. H. Wang, *Environ. Chem. Lett.* **2011**, 9, 331.
- [6] a) S. Licht, B. Wang, S. Ghosh, *Science* **1999**, 285, 1039; b) S. Wang, Y. Wang, S. Chen, H. Hou, H. Li, *Electrochim. Acta* **2016**, 213, 132.
- [7] J. Q. Jiang, *J. Chem. Technol. Biot.* **2014**, 89, 165
- [8] Z. Zhang, X. Xu, *Appl. Surf. Sci.* **2015**, 346, 520.
- [9] L. Peng, Z. Xu, Z. Liu, Y. Wei, H. Sun, Z. Li, X. Zhao, C. Gao, *Nat. Commun.* **2015**, 6, 5716.
- [10] Z. Sofer, J. Luxa, O. Jankovský, D. Sedmidubský, T. Bystroň, M. Pumera, *Angew. Chem. Int. Edit.* **2016**, 55, 11965; *Angew. Chem.* **2016**, 128, 12144.
- [11] a) Y. Jiang, J. E. Goodwill, J. E. Tobiasson, D. A. Reckhow, *Environ. Sci. Technol.* **2015**, 49, 2841; b) M. Kolar, P. Novak, K. Siskova, L. Machala, O. Malina, J. Tucek, V. K. Sharma, R. Zboril, *Phys. Chem. Chem. Phys.* **2016**, 18, 4415; c) J. M. Schroyer, L. T. Ockerman, *Anal. Chem.* **1951**, 23, 1312.
- [12] a) R. A. Sheldon, *Green Chem.* **2017**, 19, 18; b) C. M. Alder, J. D. Hayler, R. K. Henderson, A. M. Redman, L. Shukla, L. E. Shuster, H. F. Sneddon, *Green Chem.* **2016**, 18, 3879.
- [13] B. Viswanath, P. Kundu, A. Halder, N. Ravishankar, *J. Phys. Chem. C* **2009**, 113, 16866.
- [14] a) S. L. James, C. J. Adams, C. Bolm, D. Braga, P. Collier, T. Friščić, F. Grepioni, K. D. M. Harris, G. Hyett, W. Jones, A. Krebs, J. Mack, L.

- Maini, A. G. Orpen, I. P. Parkin, W. C. Shearouse, J. W. Steed, D. C. Waddell, *Chem. Soc. Rev.* **2012**, *41*, 413; b) S. E. Zhu, F. Li, G. W. Wang, *Chem. Soc. Rev.* **2013**, *42*, 7535; c) F. Hammerer, L. Loots, J. Do, J. P. D. Therien, C. W. Nickels, T. Friščić, K. Auclair, *Angew. Chem. Int. Edit.* **2018**, *57*, 2621; *Angew. Chem.* **2018**, *130*, 2651.
- [15] a) R. J. Audette, J. W. Quai, P. J. Smith, *Tetrahedron Lett.* **1971**, *12*, 279; b) Y. Tsuda, S. Nakajima, *Chem. Lett.* **1978**, *7*, 1397; c) K. S. Kim, Y. H. Song, N. H. Lee, C. S. Hahn, *Tetrahedron Lett.* **1986**, *27*, 2875.
- [16] The product information can be accessed via <http://www.timesnano.com/en/view.php?prt=3,29,50,81&id=244>.
- [17] C. Wu, D. Zheng, H. Wang, L. Guan, *ChemPlusChem* **2014**, *79*, 394.
- [18] a) R. Gusmao, Z. Sofer, M. Novacek, J. Luxa, S. Matejkova, M. Pumera, *Nanoscale* **2016**, *8*, 6700; b) A. Y. S. Eng, C. K. Chua, M. Pumera, *Nanoscale* **2015**, *7*, 20256; c) G. Shao, Y. Lu, F. Wu, C. Yang, F. Zeng, Q. Wu, *J. Mater. Sci.* **2012**, *47*, 4400; d) W. Gao, L. B. Alemany, L. Ci, P. M. Ajayan, *Nat. Chem.* **2009**, *1*, 403.
- [19] The product information can be accessed via <http://www.carbonsolution.com/products/p3-swnt>.
- [20] B. Zhao, H. Hu, A. Yu, D. Perea, R. C. Haddon, *J. Am. Chem. Soc.* **2005**, *127*, 8197.
- [21] a) K. Chun, I. Moon, J. Han, S. Do, J. Lee, S. Jeon, *Nanoscale* **2013**, *5*, 10171; b) G. U. Sumanasekera, J. L. Allen, S. L. Fang, A. L. Loper, A. M. Rao, P. C. Eklund, *J. Phys. Chem. B* **1999**, *103*, 4292.
- [22] a) H. Yu, Y. G. Jin, F. Peng, H. J. Wang, J. Yang, *J. Phys. Chem. C* **2008**, *112*, 6758. b) R. Gusmão, Z. Sofer, M. Nováček, M. Pumera, *ChemElectroChem* **2016**, *3*, 1713.

## Table of Contents

## COMMUNICATION

Ferrate(VI) under solvent-free conditions displays intrinsically strong and unexpected oxidizing power, which can be readily harnessed and promoted by mechanochemistry for green oxidative transformation of both organic and inorganic substrates.



Zhao-Yang Zhang, Deyang Ji, Wenting Mao, Yu Cui, Qing Wang, Lu Han, Hongliang Zhong, Zhongming Wei, Yixin Zhao, Kasper Nørgaard, and Tao Li\*

Page No. – Page No.

“Dry” Chemistry of Ferrate(VI): A Solvent-free Mechanochemical way for Versatile Green Oxidation